Structural Engineering and Mechanics, Vol. 22, No. 6 (2006) 701-717
DOI: http://dx.doi.org/10.12989/sem.2006.22.6.701

On the natural frequencies and mode shapes of a multiple-step beam carrying a number of intermediate lumped masses and rotary inertias

Hsien-Yuan Lin†

Department of Mechanical and Electro-Mechanical Engineering, National Sun Yat-Sen University, 70, Lien-hai Road, Kaohsiung 804, Taiwan, ROC

Ying-Chien Tsai‡

Department of Mechanical and Electro-Mechanical Engineering, National Sun Yat-Sen University, 70, Lien-hai Road, Kaohsiung 804, Taiwan, ROC
Department of Mechanical Engineering, Cheng Shiu University, Kaohsiung 833, Taiwan, ROC

(Received August 24, 2005, Accepted December 9, 2005)

Abstract. In the existing reports regarding free transverse vibrations of the Euler-Bernoulli beams, most of them studied a uniform beam carrying various concentrated elements (such as point masses, rotary inertias, linear springs, rotational springs, spring-mass systems, …, etc.) or a stepped beam with one to three step changes in cross-sections but without any attachments. The purpose of this paper is to utilize the numerical assembly method (NAM) to determine the exact natural frequencies and mode shapes of the multiple-step Euler-Bernoulli beams carrying a number of lumped masses and rotary inertias. First, the coefficient matrices for an intermediate lumped mass (and rotary inertia), left-end support and right-end support of a multiple-step beam are derived. Next, the overall coefficient matrix for the whole vibrating system is obtained using the numerical assembly technique of the conventional finite element method (FEM). Finally, the exact natural frequencies and the associated mode shapes of the vibrating system are determined by equating the determinant of the last overall coefficient matrix to zero and substituting the corresponding values of integration constants into the associated eigenfunctions, respectively. The effects of distribution of lumped masses and rotary inertias on the dynamic characteristics of the multiple-step beam are also studied.

Keywords: multiple-step beam; lumped mass; rotary inertia; exact natural frequency; mode shape; integration constants.

1. Introduction

For the (non-uniform) stepped beams, Balasubramanian and Subramanian (1985), Subramanian and Balasubramanian (1987) and Balasubramanian *et al*. (1990) investigated the free vibration characteristics of the single-step beams. Jang and Bert (1989a, 1989b) reported the exact and

† Ph.D. Student
‡ Professor, Corresponding author, E-mail: yctsai@csu.edu.tw

numerical solutions for the natural frequencies of a single-step beam under various boundary conditions. Laura *et al.* (1994) presented the experimental results for the natural frequencies of a single-step beam. Maurizi and Belles (1994) studied the natural frequencies of the one-span beams with stepwise variable cross-sections. Lee and Bergman (1994) used the elemental dynamic flexibility method to study the free and forced vibrations of the seven-step beam. Ju *et al.* (1994) used a first order shear deformation theory and the corresponding finite element formulation to analyze the free vibration of two-step beams. De Rosa (1994) and De Rosa *et al.* (1995) deduced the free vibration frequencies of a single-step beam by solving the differential equations of motion and the associated eigenvalues. Naguleswaran found the natural frequencies and mode shapes of an Euler-Bernoulli beam on classical end supports and with one-step change in cross-section by equating the second order determinant to zero (2002a), and also the natural frequencies of an Euler-Bernoulli beam on elastic end supports and with up to three-step changes in cross-sections by equating the fourth order determinant to zero (2002b).

For the uniform beams, Hamdan and Abdel (1994) found the exact natural frequencies of a uniform beam with attached inertia elements. Wu and Chou (1998) found the approximate natural frequencies and mode shapes of a uniform beam carrying any number of elastically attached lumped masses by means of the analytical-and-numerical-combined method (ANCM). Later, Wu and Chou (1999) obtained the exact solution of the similar vibrating system by using the numerical assembly method (NAM). By means of the same method (NAM), Wu and Chen (2001) studied the free vibration characteristics of a uniform Timoshenko beam carrying multiple spring-mass systems, Chen and Wu (2002) and Chen (2003) obtained the exact solutions for the natural frequencies and mode shapes of the non-uniform (wedge) beams carrying multiple spring-mass system or other various concentrated elements. Recently, Lin and Tsai (2005) successfully determined the exact values of natural frequencies and the associated mode shapes of a multi-span uniform beam carrying a number of point masses with the same NAM.

From the above literature review one sees that the exact solutions for the natural frequencies and mode shapes of a single-step beam carrying either single or multiple lumped masses or a multiple-step beam without any attachments have been obtained. However, little was found in the literature regarding the exact solutions for the natural frequencies and mode shapes of a multiple-step beam carrying either single or multiple lumped masses and rotary inertias. Therefore, this paper adopts the numerical assembly method (NAM) to investigate the free vibration characteristics of a multiple-step beam carrying a number of lumped masses and rotary inertias.

2. Equation of motion and displacement function

Fig. 1 shows the sketch of a pinned-pinned beam with S-step changes in cross-sections and carrying K lumped masses and R rotary inertias. The points corresponding to the locations of the S-step changes in cross-sections, K lumped masses or R rotary inertias are referred to as "stations". Where $m_k (k = 1 \sim K)$ is the lumped mass (●), $J_r (r = 1 \sim R)$ is the rotary inertia, $s_s (s = 1 \sim S)$ is the numbering for the step change in cross-section and N is the total number of stations. Clearly, the total number of stations is given by $N = S + K + R - H$ with H denoting the total number of overlapped stations for step changes in cross-sections, lumped masses and/or rotary inertias. In other words, H is the difference between $(S + K + R)$ and the total number of stations occupied by all the step changes in cross-sections, lumped masses and/or rotary inertias, N.

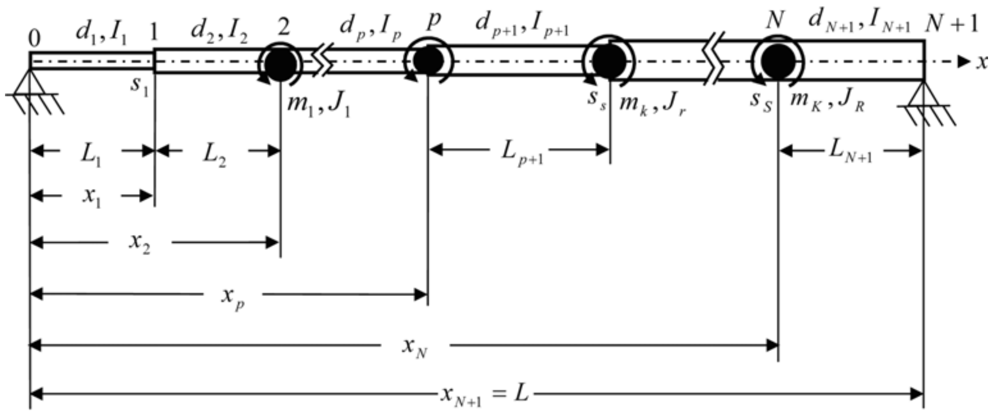

Fig. 1 Sketch for a pinned-pinned beam with S-step changes in cross-sections and carrying K lumped masses and R rotary inertias

The differential equation of motion for the i-th beam segment is given by

$$EI_i \frac{\partial^4 y_i(x, t)}{\partial x^4} + \overline{m}_i \frac{\partial^2 y_i(x, t)}{\partial^2 t} = 0 \qquad i = 1, 2, \ldots, N, N+1 \tag{1}$$

where E is Young's modulus, I_i is moment of inertia of the cross-sectional area of the beam segment i, $\overline{m}_i$ is the mass per unit length of the beam segment i, and $y_i(x, t)$ is the transverse displacement at position x and time t shown in Fig. 1.

For free vibration one has

$$y_i(x, t) = Y_i(x) e^{j\omega t} \tag{2}$$

where $Y_i(x)$ is the amplitude of $y_i(x, t)$, ω is the natural frequency of the beam, and $j = \sqrt{-1}$.

Substitution of Eq. (2) into Eq. (1) gives:

$$Y_i'''' - \beta_{v,i}^4 Y_i = 0 \tag{3}$$

where

$$\beta_{v,i}^4 = \frac{\omega_v^2 \overline{m}_i}{EI_i} \tag{4a}$$

or

$$\omega_v = (\beta_{v,i} L)^2 \left(\frac{EI_i}{\overline{m}_i L^4}\right)^{1/2} = \Omega_{v,i}^2 \left(\frac{EI_i}{\overline{m}_i L^4}\right)^{1/2} \tag{4b}$$

with

$$\Omega_{v,i} = \beta_{v,i} L \tag{4c}$$

In Eqs. (4a) to (4c), the subscripts v and i denote the v-th vibration mode and i-th beam segment, respectively.

The solution of Eq. (3) takes the form:

$$Y_i(x) = C_{i,1}\sin\beta_{v,i}x + C_{i,2}\cos\beta_{v,i}x + C_{i,3}\sinh\beta_{v,i}x + C_{i,4}\cosh\beta_{v,i}x \tag{5}$$

Which represents the displacement function for the i-th beam segment located at the left side of i-th station.

3. Determination of the natural frequencies and mode shapes

At the arbitrary station p located at $x = x_p$ (see Fig. 1), from Eq. (5) one has

$$Y_p(\xi_p) = C_{p,1}\sin\Omega_{v,p}\xi_p + C_{p,2}\cos\Omega_{v,p}\xi_p + C_{p,3}\sinh\Omega_{v,p}\xi_p + C_{p,4}\cosh\Omega_{v,p}\xi_p \tag{6}$$

$$Y_p'(\xi_p) = \Omega_{v,p}(C_{p,1}\cos\Omega_{v,p}\xi_p - C_{p,2}\sin\Omega_{v,p}\xi_p + C_{p,3}\cosh\Omega_{v,p}\xi_p + C_{p,4}\sinh\Omega_{v,p}\xi_p) \tag{7}$$

$$Y_p''(\xi_p) = \Omega_{v,p}^2(-C_{p,1}\sin\Omega_{v,p}\xi_p - C_{p,2}\cos\Omega_{v,p}\xi_p + C_{p,3}\sinh\Omega_{v,p}\xi_p + C_{p,4}\cosh\Omega_{v,p}\xi_p) \tag{8}$$

$$Y_p'''(\xi_p) = \Omega_{v,p}^3(-C_{p,1}\cos\Omega_{v,p}\xi_p + C_{p,2}\sin\Omega_{v,p}\xi_p + C_{p,3}\cosh\Omega_{v,p}\xi_p + C_{p,4}\sinh\Omega_{v,p}\xi_p) \tag{9}$$

with

$$\xi_p = \frac{x_p}{L} \tag{10}$$

In Eqs. (7), (8) and (9), the primes refer to differentiation with respect to the coordinate x and $\Omega_{v,p}$ represents the dimensionless frequency parameter for the p-th beam segment corresponding to the v-th vibration mode.

The continuity of deformations and the equilibrium of moments and forces require that:

$$Y_p(\xi_p) = Y_{p+1}(\xi_p) \tag{11a}$$

$$Y_p'(\xi_p) = Y_{p+1}'(\xi_p) \tag{11b}$$

$$Y_p''(\xi_p) - \Omega_{v,p}^4 J_p^*\left(\frac{\overline{m}_1}{\overline{m}_p}\right) Y_p'(\xi_p) = \varepsilon_p Y_{p+1}''(\xi_p) \tag{11c}$$

$$Y_p'''(\xi_p) + \Omega_{v,p}^4 m_p^*\left(\frac{\overline{m}_1}{\overline{m}_p}\right) Y_p(\xi_p) = \varepsilon_p Y_{p+1}'''(\xi_p) \tag{11d}$$

with

$$m_p^* = \frac{m_p}{\overline{m}_1 L}, \quad J_p^* = \frac{J_p}{\overline{m}_1 L^3}, \quad \varepsilon_p = \frac{I_{p+1}}{I_p} \tag{12a-c}$$

m_p and J_p are respectively the p-th lumped mass and rotary inertia, while $\overline{m}_1$ and $\overline{m}_p$ denote the mass per unit length of the 1st and p-th beam segment respectively.

Substitution of Eqs. (6)-(9) into Eqs. (11a)-(11d) leads to

$$C_{p,1}\sin\Omega_{v,p}\xi_p + C_{p,2}\cos\Omega_{v,p}\xi_p + C_{p,3}\sinh\Omega_{v,p}\xi_p + C_{p,4}\cosh\Omega_{v,p}\xi_p$$
$$-C_{p+1,1}\sin\Omega_{v,p+1}\xi_p - C_{p+1,2}\cos\Omega_{v,p+1}\xi_p - C_{p+1,3}\sinh\Omega_{v,p+1}\xi_p - C_{p+1,4}\cosh\Omega_{v,p+1}\xi_p = 0 \quad (13a)$$

$$\Omega_{v,p}(C_{p,1}\cos\Omega_{v,p}\xi_p - C_{p,2}\sin\Omega_{v,p}\xi_p + C_{p,3}\cosh\Omega_{v,p}\xi_p + C_{p,4}\sinh\Omega_{v,p}\xi_p)$$
$$-\Omega_{v,p+1}(C_{p,1}\cos\Omega_{v,p+1}\xi_p - C_{p,2}\sin\Omega_{v,p+1}\xi_p + C_{p,3}\cosh\Omega_{v,p+1}\xi_p + C_{p,4}\sinh\Omega_{v,p+1}\xi_p) = 0 \quad (13b)$$

$$\Omega^2_{v,p}(-C_{p,1}\sin\Omega_{v,p}\xi_p - C_{p,2}\cos\Omega_{v,p}\xi_p + C_{p,3}\sinh\Omega_{v,p}\xi_p + C_{p,4}\cosh\Omega_{v,p}\xi_p)$$
$$-J^*_p\Omega^5_{v,p}\left(\frac{\overline{m}_1}{\overline{m}_p}\right)(C_{p,1}\cos\Omega_{v,p}\xi_p - C_{p,2}\sin\Omega_{v,p}\xi_p + C_{p,3}\cosh\Omega_{v,p}\xi_p + C_{p,4}\sinh\Omega_{v,p}\xi_p)$$
$$-\varepsilon_p\Omega^2_{v,p+1}(-C_{p+1,1}\sin\Omega_{v,p+1}\xi_p - C_{p+1,2}\cos\Omega_{v,p+1}\xi_p + C_{p+1,3}\sinh\Omega_{v,p+1}\xi_p + C_{p+1,4}\cosh\Omega_{v,p+1}\xi_p) = 0 \quad (13c)$$

$$\Omega^3_{v,p}(-C_{p,1}\cos\Omega_{v,p}\xi_p + C_{p,2}\sin\Omega_{v,p}\xi_p + C_{p,3}\cosh\Omega_{v,p}\xi_p + C_{p,4}\sinh\Omega_{v,p}\xi_p)$$
$$+m^*_p\Omega^4_{v,p}\left(\frac{\overline{m}_1}{\overline{m}_p}\right)(C_{p,1}\sin\Omega_{v,p}\xi_p + C_{p,2}\cos\Omega_{v,p}\xi_p + C_{p,3}\sinh\Omega_{v,p}\xi_p + C_{p,4}\cosh\Omega_{v,p}\xi_p)$$
$$-\varepsilon_p\Omega^3_{v,p+1}(-C_{p+1,1}\cos\Omega_{v,p+1}\xi_p + C_{p+1,2}\sin\Omega_{v,p+1}\xi_p + C_{p+1,3}\cosh\Omega_{v,p+1}\xi_p + C_{p+1,4}\sinh\Omega_{v,p+1}\xi_p) = 0 \quad (13d)$$

Writing Eqs. (13a)-(13d) in matrix form, one has

$$[B_p]\{C_p\} = 0 \quad (14)$$

where

$$\{C_p\} = \{C_{p,1}\ \ C_{p,2}\ \ C_{p,3}\ \ C_{p,4}\ \ C_{p+1,1}\ \ C_{p+1,2}\ \ C_{p+1,3}\ \ C_{p+1,4}\} \quad (15)$$

and the coefficient matrix $[B_p]$ is placed in Appendix at the end of this paper.

If the left-end support of the beam is pinned (as shown in Fig. 1), then the boundary conditions are:

$$Y_0(0) = Y''_0(0) = 0 \quad (16a,b)$$

From Eqs. (6), (8) and (16), it can be shown that

$$C_{1,2} + C_{1,4} = 0 \quad (17a)$$

$$-C_{1,2} + C_{1,4} = 0 \quad (17b)$$

or in matrix form

$$[B_L]\{C_L\} = 0 \quad (18)$$

where:

$$[B_L] = \begin{array}{c} \begin{array}{cccc} 1 & 2 & 3 & 4 \end{array} \\ \begin{bmatrix} 0 & 1 & 0 & 1 \\ 0 & -1 & 0 & 1 \end{bmatrix} \end{array} \begin{array}{c} \\ 1 \\ 2 \end{array} \tag{19}$$

$$\{C_L\} = \{C_{1,1} \;\; C_{1,2} \;\; C_{1,3} \;\; C_{1,4}\} \tag{20}$$

Similarly, if the right-end support of the beam is pinned, then the boundary conditions are given by

$$Y_{N+1}(L) = Y''_{N+1}(L) = 0 \tag{21a,b}$$

Substituting Eqs. (6) and (8) into Eq. (21) gives

$$C_{N+1,1}\sin\Omega_{v,N+1} + C_{N+1,2}\cos\Omega_{v,N+1} + C_{N+1,3}\sinh\Omega_{v,N+1} + C_{N+1,4}\cosh\Omega_{v,N+1} = 0 \tag{22a}$$

$$-C_{N+1,1}\sin\Omega_{v,N+1} - C_{N+1,2}\cos\Omega_{v,N+1} + C_{N+1,3}\sinh\Omega_{v,N+1} + C_{N+1,4}\cosh\Omega_{v,N+1} = 0 \tag{22b}$$

or

$$[B_R]\{C_R\} = 0 \tag{23}$$

where

$$[B_R] = \begin{array}{c} \begin{array}{cccc} 4N+1 & 4N+2 & 4N+3 & 4N+4 \end{array} \\ \begin{bmatrix} \sin\Omega_{v,N+1} & \cos\Omega_{v,N+1} & \sinh\Omega_{v,N+1} & \cosh\Omega_{v,N+1} \\ -\sin\Omega_{v,N+1} & -\cos\Omega_{v,N+1} & \sinh\Omega_{v,N+1} & \cosh\Omega_{v,N+1} \end{bmatrix} \end{array} \begin{array}{c} \\ q-1 \\ q \end{array} \tag{24}$$

$$\{C_R\} = \{C_{N+1,1} \;\; C_{N+1,2} \;\; C_{N+1,3} \;\; C_{N+1,4}\} \tag{25}$$

For a cantilever beam, the boundary conditions are given by

$$Y_0(0) = Y'_0(0) = 0 \tag{26a,b}$$

$$Y''_{N+1}(L) = Y'''_{N+1}(L) = 0 \tag{27a,b}$$

From Eqs. (6), (7), (8), (9), (26) and (27), one obtains the following boundary coefficient matrices

$$[B_L] = \begin{array}{c} \begin{array}{cccc} 1 & 2 & 3 & 4 \end{array} \\ \begin{bmatrix} 0 & 1 & 0 & 1 \\ 1 & 0 & 1 & 0 \end{bmatrix} \end{array} \begin{array}{c} \\ 1 \\ 2 \end{array} \tag{28}$$

$$[B_R] = \begin{array}{c} \begin{array}{cccc} 4N+1 & 4N+2 & 4N+3 & 4N+4 \end{array} \\ \begin{bmatrix} -\sin\Omega_{v,N+1} & -\cos\Omega_{v,N+1} & \sinh\Omega_{v,N+1} & \cosh\Omega_{v,N+1} \\ -\cos\Omega_{v,N+1} & \sin\Omega_{v,N+1} & \cosh\Omega_{v,N+1} & \sinh\Omega_{v,N+1} \end{bmatrix} \end{array} \begin{array}{c} \\ q-1 \\ q \end{array} \tag{29}$$

For a free-clamped beam, the boundary conditions are given by

$$Y_0''(0) = Y_0'''(0) = 0 \tag{30a,b}$$

$$Y_{N+1}(L) = Y_{N+1}'(L) = 0 \tag{31a,b}$$

From Eqs. (6), (7), (8), (9), (30) and (31), one has the associated boundary coefficient matrices

$$[B_L] = \begin{array}{c} \begin{array}{cccc} 1 & 2 & 3 & 4 \end{array} \\ \begin{bmatrix} 0 & -1 & 0 & 1 \\ -1 & 0 & 1 & 0 \end{bmatrix} \end{array} \begin{array}{c} \\ 1 \\ 2 \end{array} \tag{32}$$

$$[B_R] = \begin{array}{c} \begin{array}{cccc} 4N+1 & 4N+2 & 4N+3 & 4N+4 \end{array} \\ \begin{bmatrix} \sin\Omega_{v,N+1} & \cos\Omega_{v,N+1} & \sinh\Omega_{v,N+1} & \cosh\Omega_{v,N+1} \\ \cos\Omega_{v,N+1} & -\sin\Omega_{v,N+1} & \cosh\Omega_{v,N+1} & \sinh\Omega_{v,N+1} \end{bmatrix} \end{array} \begin{array}{c} \\ q-1 \\ q \end{array} \tag{33}$$

In the foregoing equations, N denotes the total number of intermediate stations (see Fig. 1) and q denotes the total number of equations for the integration constants. They have the following relationship

$$q = 4N + 4 \tag{34}$$

From the above derivations, it is evident that one may obtain four equations from each intermediate station. In addition, one may obtain two equations from the left-end station and the right-end station of the beam, respectively. Therefore, the total number of equations q is given by Eq. (34): $q = 4N + 4$.

The integration constants relating to the left-end support and those relating to the right-end support of the beam are determined by Eqs. (18) and (23), respectively, while those relating to the intermediate stations (i.e., 1 to N) are determined by Eq. (14). The associated coefficient matrices are given by $[B_L]$, $[B_p]$, $[B_R]$ as may be seen from Eqs. (19), (A1) (in Appendix) and (24), respectively. In the last three equations, the identification number for each element of the last three coefficient matrices is indicated at the top side and right side of each matrix. Therefore, using the numerical assembly technique as done by the conventional finite element method, an equation for all the integration constants of the entire beam can be obtained, i.e.,

$$[\overline{B}]\{\overline{C}\} = 0 \tag{35}$$

Non-trivial solution of Eq. (35) requires that:

$$|\overline{B}| = 0 \tag{36}$$

Which is the frequency equation for the present problem.

In this paper, the half-interval method (Epperson 2003) is used to determine the natural frequencies of a beam with S-step changes in cross-sections, carrying K lumped masses and R rotary inertias, ω_v ($v = 1, 2, \ldots$). For each natural frequency ω_v, the corresponding integration constants can be obtained from Eq. (35). Substitution of these integration constants into the displacement functions of the associated beam segments will yield the corresponding mode shape of the beam.

Table 1 Five lowest five frequency parameters of the uniform cantilever beam carrying two lumped masses and rotary inertias with $m_1^* = 5.0$, $J_1^* = 1.0$ at $\xi_1 = 0.5$, and $m_2^* = 5.0$, $J_2^* = 1.0$ at $\xi_2 = 1.0$ (Example 1)

Methods	Frequency parameters, $\Omega_{v,1} = \left(\omega_v\sqrt{\bar{m}_1 L^4/(EI_1)}\right)^{1/2}$				
	$\Omega_{1,1}$	$\Omega_{2,1}$	$\Omega_{3,1}$	$\Omega_{4,1}$	$\Omega_{5,1}$
Present	0.752515	1.383354	2.137078	2.708819	9.480262
Hamdan and Abdel (1994)	0.752515	1.383353	2.137078	2.708818	9.480262

4. Numerical results and discussions

Before performing the free vibration analysis of a beam with S-step changes in cross-sections, carrying K lumped masses and R rotary inertias, the reliability of the theory and computer program developed for this paper are confirmed by comparing the present results with those obtained from the existing literature or the conventional finite element method (FEM). Here, the two-node beam elements are used in the FEM and the entire beam is subdivided into 40 beam elements. Since each node has two degrees of freedom (DOF's), the total DOF for the entire beam is given by $2(40 + 1) = 82$.

4.1 Reliability of the developed computer program

The first example studied in this paper is a uniform cantilever beam carrying two lumped masses: the first one is m_1 with rotary inertia J_1 located at an intermediate point $\xi_1 = x_1/L = 0.5$, and the second one is m_2 with rotary inertia J_2 at the free end $\xi_2 = x_2/L = 1.0$. The corresponding dimensionless parameters are

$$m_1^* = \frac{m_1}{\bar{m}_1 L} = 5.0,\quad J_1^* = \frac{J_1}{\bar{m}_1 L^3} = 1.0,\quad m_2^* = \frac{m_2}{\bar{m}_1 L} = 5.0,\quad J_2^* = \frac{J_2}{\bar{m}_1 L^3} = 1.0,\quad \varepsilon_1 = \frac{EI_2}{EI_1} = 1$$

Table 1 shows the lowest five frequency parameters of the beam, $\Omega_{v,1} = \left(\omega_v\sqrt{\bar{m}_1 L^4/(EI_1)}\right)^{1/2}$ ($v = 1$ to 5). It is seen that the current numerical results are in good agreement with those given by Hamdan and Abdel (1994).

The second example studied is a pinned-pinned beam with three-step changes in cross sections located at $\xi_1 = 0.25$, $\xi_2 = 0.55$ and $\xi_3 = 0.80$, respectively. It is evident that a three-step beam is composed of four beam segments. Three types of cross-sections for the four beam segments are investigated. For the first type, the four beam segments have the same depths h but different widths b_i ($i = 1$ to 4), so that

$$\varepsilon_i = \frac{E_i I_i}{E_1 I_1} = \frac{b_i}{b_1} = 1.0,\ 0.8,\ 0.65,\ 0.25 \text{ (first type)} \tag{37}$$

The second type of the stepped beam is similar to the first one, the only difference is that the four beam segments have the same widths b but different depths h_i ($i = 1$ to 4), so that

$$\varepsilon_i = \frac{E_i I_i}{E_1 I_1} = \left(\frac{h_i}{h_1}\right)^3 = 1.0,\ (0.8)^3,\ (0.65)^3,\ (0.25)^3 \quad \text{(second type)} \tag{38}$$

Table 2 The lowest five frequency parameters of the pinned-pinned beam with three-step changes in cross sections, $\Omega_{v,1} = (\omega_v\sqrt{\bar{m}_1 L^4/(EI_1)})^{1/2}$ (v = 1 to 5)

Stepped beams	Methods	Frequency parameters, $\Omega_{v,1} = \left(\omega_v\sqrt{\bar{m}_1 L^4/(EI_1)}\right)^{1/2}$				
		$\Omega_{1,1}$	$\Omega_{2,1}$	$\Omega_{3,1}$	$\Omega_{4,1}$	$\Omega_{5,1}$
Type 1	Present	3.09682	6.18383	9.34252	12.60534	15.81630
cf. Eq. (37)	Naguleswaran (2002b)	3.09682	6.18383	9.34252	-	-
Type 2	Present	2.24074	4.63823	7.43284	9.92892	11.81239
cf. Eq. (38)	Naguleswaran (2002b)	2.24074	4.63823	7.43284	-	-
Type 3	Present	1.88817	4.61149	7.60874	9.89280	11.67232
cf. Eq. (39)	Naguleswaran (2002b)	1.88817	4.61149	7.60874	-	-

For the third type of the stepped beam, the four beam segments have circular cross-sections with diameters d_i (i = 1 to 4), so that

$$\varepsilon_i = \frac{E_i I_i}{E_1 I_1} = \left(\frac{d_i}{d_1}\right)^4 = 1.0,\ (0.8)^4,\ (0.65)^4,\ (0.25)^4 \quad \text{(third type)} \tag{39}$$

In Eqs. (37)-(39), it has been assumed that the materials of the four beam segments are the same, i.e., $E_i = E_1$ (i = 1 to 4). Table 2 shows the lowest five frequency parameters of the three-step beam, $\Omega_{v,1} = (\omega_v\sqrt{\bar{m}_1 L^4/(EI_1)})^{1/2}$ (v = 1 to 5). It is seen that the current numerical results are also in good agreement with those of Naguleswaran (2002b).

4.2 A three-step beam with single lumped mass m_1

The current Example 3 studies the case of a three-step beam with circular cross-sections (with diameter ratios $d_i^* = d_i/d_1$ = 1.0, 1.5, 2.0 and 3.0) and carrying a lumped mass m_1 = 0.45 × 15.3875 = 6.924375 kg. The three-step changes in cross-sections are located at ξ_1 = 0.20, ξ_2 = 0.50 and ξ_3 = 0.75, respectively. Three types of boundary conditions (P-P, C-F and F-C) along with the next five cases are investigated: (m_1^*=0.45, ξ_1 = 0.35), (m_1^* = 0.45, ξ_1 = 0.60) and (m_1^* = 0.45, ξ_1 = 0.90). Where P, C and F represent the abbreviations of pinned, clamped and free, respectively.

The dimensions of the three-step beam for the finite element analysis are shown in Fig. 2. From the figure one sees that d_1 = 0.05 m, d_2 = 0.075 m, d_3 = 0.10 m and d_4 = 0.15 m; L_1 = 0.2 m, L_2 = 0.3 m, L_3 = 0.25 m and L_4 = 0.25 m. It is evident that the total length of the stepped beam is $L = L_1 + L_2 + L_3 + L_4$ = 1.0 m; the locations for the step changes in cross-sections are ξ_1 = 0.20, ξ_2 = 0.50 and ξ_3 = 0.75; the diameter ratios are $d_i^* = d_i/d_1$ = 1.0, 1.5, 2.0 and 3.0. For the four uniform beam segments, the cross-sectional areas are: $A_i = \pi d_i^2/4$ = 1.9635 × 10^{-4}, 44.17875 × 10^{-4}, 78.540 × 10^{-4} and 176.715 × 10^{-4} m^2; the area moments of inertia are: $I_i = \pi d_i^4/64$ = 3.067969 × 10^{-7}, 15.53159 × 10^{-7}, 49.0875 × 10^{-7} and 248.50547 × 10^{-7} m^4; the mass per unit length are: $\bar{m}_i = \rho A_i$ = 15.38756, 34.6220, 61.55023 and 138.4880 kg/m with mass density ρ = 7.8368 × 10^3 kg/m^3. Besides, the Young's modulus is E = 2.069 × 10^{11} N/m^2. The reference mass is $\bar{m}_1 L$ = 15.38756 kg and the reference rotary is $\bar{m}_1 L^3$ = 15.38756 kg-m^2. Each beam segment is subdivided into ten beam elements; therefore, the lengths for each beam element in each beam segment are 0.02, 0.03, 0.025 and 0.025 m, respectively.

Table 3 shows the effect of locations of the single lumped mass m_1 on the lowest five natural

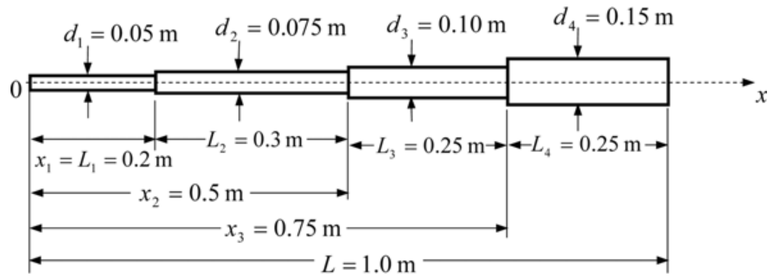

Fig. 2 The dimensions of the three-step beam for the finite element analysis

Table 3 The lowest five natural frequencies, ω_v (v = 1 to 5), of the *stepped* beam with three changes in cross-sections at $\xi_i = 0.20$, 0.50 and 0.75, respectively, and diameter ratios $d_i^* = d_i/d_1$ = 1.0, 1.5, 2.0 and 3.0, carrying a lumped mass m_1 = 6.924375 kg

Boundary conditions	ξ_1	Methods	Natural frequencies, ω_v (rad/sec)				
			ω_1	ω_2	ω_3	ω_4	ω_5
P-P	*	Present	892.7602	4024.4722	9293.2685	18128.6892	27828.3603
		FEM	892.7596	4024.4722	9293.2896	18128.8626	27829.0470
	0.35	Present	782.2295	3744.5658	8733.2095	16325.5368	27356.3545
		FEM	782.2244	3744.5427	8733.1699	16325.5208	27356.8624
	0.60	Present	814.8855	3895.4797	9262.9433	16943.4370	26259.2843
		FEM	814.8802	3895.4562	9262.9043	16943.4544	26259.7265
	0.90	Present	886.4703	3983.8521	9147.6858	17817.2618	27010.3220
		FEM	886.4646	3983.8274	9147.6480	17817.3103	27010.7490
C-F	*	Present	103.3811	1652.2970	5919.9740	11924.6451	21941.7090
		FEM	103.3809	1652.2960	5919.9785	11924.6964	21942.0237
	0.35	Present	102.6549	1427.9478	5409.7267	11440.0148	19430.3791
		FEM	102.6542	1427.9392	5409.6945	11439.9872	19430.4076
	0.60	Present	100.2587	1533.2898	5668.6573	11924.1645	20764.9942
		FEM	100.2580	1533.2801	5668.6265	11924.1392	20765.0905
	0.90	Present	95.4624	1627.4501	5896.3799	11916.6307	21937.6118
		FEM	95.4619	1627.4396	5896.3477	11916.6065	21937.7862
F-C	*	Present	1018.2807	3469.5860	7309.9117	12695.6389	22027.8868
		FEM	1018.2734	3469.5625	7309.8727	12695.6118	22028.0544
	0.35	Present	912.3872	3163.8253	7021.6204	12082.6956	19666.4953
		FEM	912.3813	3163.8052	7021.5817	12082.6655	19666.5255
	0.60	Present	1008.8454	3216.6350	6827.7898	12635.4980	21031.0933
		FEM	1008.8388	3216.6148	6827.7548	12635.4773	21031.1883
	0.90	Present	1018.2541	3467.7555	7293.1052	12612.0217	21837.7789
		FEM	1018.2474	3467.7331	7293.0666	12611.9953	21837.9381

*For the case of $m_1 = 0$.

frequencies of the three-step beam, ω_v (v = 1 to 5). In addition to the NAM results, Table 3 also shows the FEM results for comparisons. It is observed that an excellent agreement exists between the two sets of results. Besides, the lowest five natural frequencies of the C-F beam are much smaller than those of the F-C beam. This is a reasonable result, because the cross-section of fixed end of the C-F beam is much smaller than that of the F-C beam, for the stepped beam shown in Fig. 2.

4.3 A three-step beam with single rotary inertia J_1

The stepped beam studied in this Example 4 is the same as that studied in the last subsection, the main difference is to replace the single lumped mass m_1 by a single rotary inertia $J_1 = 0.036$

Table 4 The key is the same as Table 3 except that the three-step beam carries a rotary inertia $J_1 = 0.55395$ kg-m^2 (rather than a point mass m_1 = 6.924375 kg in Table 3)

Boundary conditions	ξ_1	Methods	Natural frequencies, ω_v (rad/sec)				
			ω_1	ω_2	ω_3	ω_4	ω_5
P-P	*	Present	892.7602	4024.4722	9293.2685	18128.6892	27828.3603
		FEM	892.7596	4024.4722	9293.2896	18128.8626	27829.0470
	0.35	Present	889.4110	2354.2254	6032.1707	12427.5750	19264.7953
		FEM	889.4053	2354.2128	6032.1359	12427.5493	19264.8485
	0.60	Present	866.5694	3595.9460	5627.8557	14452.8111	20352.4452
		FEM	866.5638	3595.9244	5627.8259	14452.8237	20352.4521
	0.90	Present	845.8443	3763.2070	8584.0825	17017.5446	25383.1700
		FEM	845.8386	3763.1841	8584.0447	17017.5738	25383.4407
C-F	*	Present	103.3811	1652.2970	5919.9740	11924.6451	21941.7090
		FEM	103.3809	1652.2960	5919.9785	11924.6964	21942.0237
	0.35	Present	102.3529	1610.9016	3018.7304	7700.1450	15900.5995
		FEM	102.3522	1610.8910	3018.7145	7700.1052	15900.6236
	0.60	Present	102.1794	1500.0450	5227.3188	6950.8433	16948.3215
		FEM	102.1788	1500.0357	5227.2887	6950.8110	16948.3977
	0.90	Present	102.1571	1404.2976	4898.3108	9891.9714	18948.9587
		FEM	102.1564	1404.2890	4898.2843	9891.9373	18949.0352
F-C	*	Present	1018.2740	3469.5633	7309.8641	12695.5561	22027.7432
		FEM	1018.2734	3469.5625	7309.8727	12695.6118	22028.0544
	0.35	Present	874.7045	2845.0017	4553.1555	9129.4597	15937.9035
		FEM	874.6989	2844.9845	4553.1282	9129.4145	15937.9271
	0.60	Present	984.3559	3079.4409	6558.0353	7501.8218	17055.6732
		FEM	984.3493	3079.4217	6557.9981	7501.7867	17055.7516
	0.90	Present	1017.4840	3414.2212	6816.2072	10979.1324	18997.5151
		FEM	1017.4771	3414.1990	6816.1713	10979.0971	18997.5742

*For the case of $J_1 = 0$.

Table 5 The key is the same as Table 3 or Table 4 except that the three-step beam carries three identical lumped masses ($m_1 = m_2 = m_3 = 6.924375$ kg) and/or three identical rotary inertias ($J_1 = J_2 = J_3 = 0.55395$ kg-m^2) located at $\xi_i = 0.35$, 0.60 and 0.90 (rather than a point mass $m_1 = 6.924375$ kg in Table 3 or a rotary inertia $J_1 = 0.55395$ kg-m^2 in Table 4)

Boundary conditions	Attachments m_k, J_r ($k = r = 1$–3)	Methods	Natural frequencies, ω_v (rad/sec)				
			ω_1	ω_2	ω_3	ω_4	ω_5
P-P	m_k^*	Present	725.5306	3527.7376	8621.0478	14820.6004	25705.7543
		FEM	725.5261	3527.7166	8621.0094	14820.5576	25706.1607
	m_k^*, J_r^*	Present	685.8376	2237.3394	3771.3942	8960.8442	12288.7630
		FEM	685.8333	2237.3275	3771.3740	8960.8024	12288.7313
C-F	m_k^*	Present	92.4594	1332.3890	5024.9443	11426.3057	18565.7008
		FEM	92.4589	1332.3809	5024.9152	11426.2784	18565.6932
	m_k^*, J_r^*	Present	90.0470	1120.2259	2867.1507	4124.3826	9165.7599
		FEM	90.0464	1120.2196	2867.1356	4124.3611	9165.7186
F-C	m_k^*	Present	905.0332	3007.4001	6370.6800	11951.7122	18764.6077
		FEM	905.0278	3007.3810	6370.6445	11951.6854	18764.5978
	m_k^*, J_r^*	Present	787.8089	2268.3714	4421.2847	5681.5942	9263.2874
		FEM	787.8045	2268.3586	4421.2589	5681.5628	9263.2458

$\times\, 15.3875 = 0.55395$ kg-m^2 located at $\xi_1 = 0.35$, 0.60 and 0.90, respectively. Table 4 shows the effect of the locations of the single rotary inertia J_1 on the lowest five natural frequencies of the three-step beam, ω_v ($v = 1$ to 5). It is obvious that the results of this paper (obtained from NAM) are in good agreement with those from FEM.

4.4 A three-step beam carrying three lumped masses and/or three rotary inertias

The final Example 5 studies the three-step beam as shown in Fig. 2 to carry three identical lumped masses and/or three rotary inertias. Three types of boundary conditions (P-P, C-F and F-C) along with the next two cases are studied: (i) The beam carries three identical lumped masses ($m_1 = m_2 = m_3 = 6.924375$ kg) only; (ii) The beam carries three identical lumped masses ($m_1 = m_2 = m_3 = 6.924375$ kg) together with three identical rotary inertias ($J_1 = J_2 = J_3 = 0.55395$ kg-m^2). In each case, the locations for the three lumped masses and/or three rotary inertias are: $\xi_1 = 0.35$, $\xi_2 = 0.60$ and $\xi_3 = 0.90$, respectively; the non-dimensional lumped masses are: $m_k^* = m_k/(\overline{m}_1 L) = 0.45$ ($k = 1, 2, 3$); while the non-dimensional rotary inertias are: $J_r^* = J_r/(\overline{m}_1 L^3) = 0.036$ ($r = 1, 2, 3$). The lowest five natural frequencies of the three-step beam, ω_v ($v = 1$ to 5), are shown in Table 5. It is seen that the results of the present paper are in good agreement with those of FEM, and the rotary inertias have significant influence on the lowest five natural frequencies of the P-P, C-F or F-C beam.

4.5 Mode shapes of the uniform and stepped beams

Figs. 3(a)-3(d) show the lowest five mode shapes of the P-P beam. Among which, the 1st, 2nd,

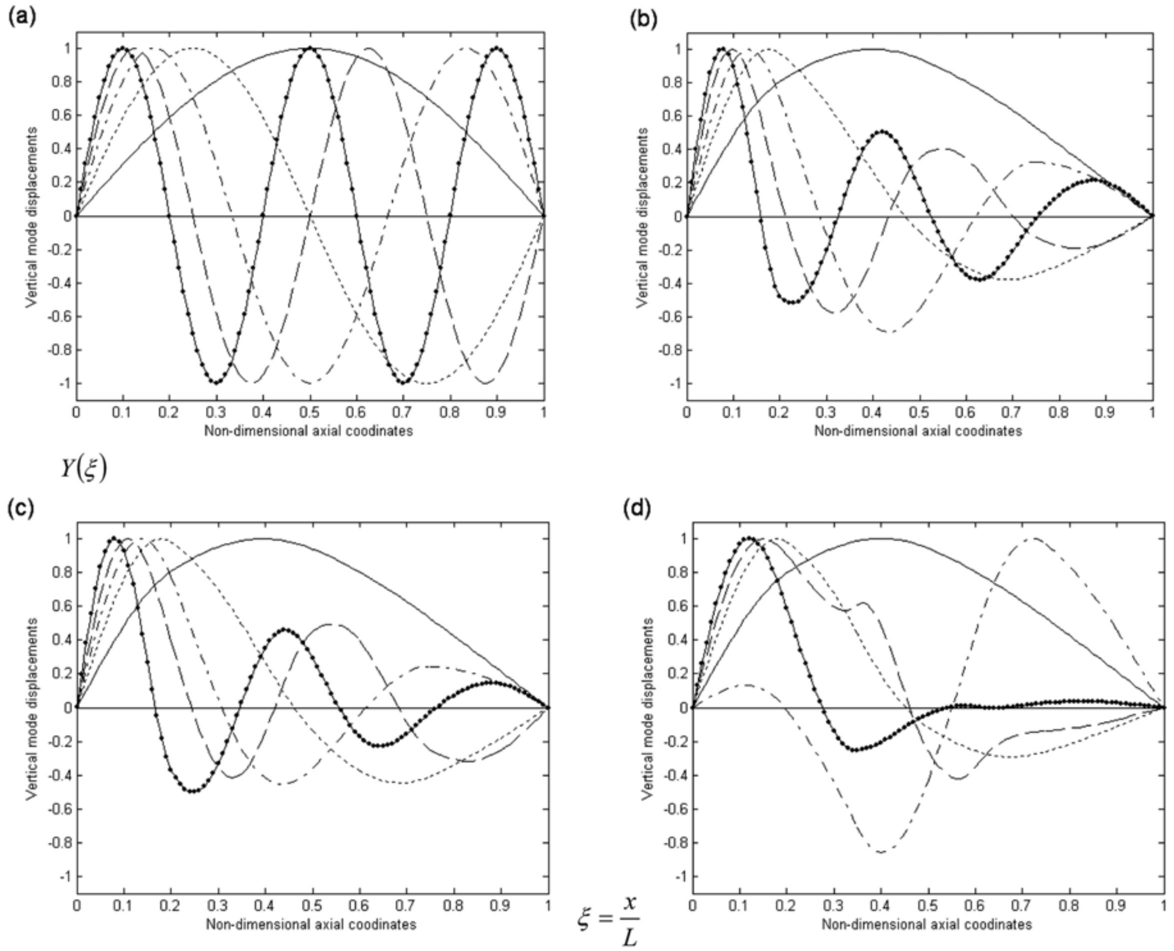

Fig. 3 The lowest five mode shapes of the P-P (pinned-pinned) beam with the 1st, 2nd, 3rd, 4th and 5th mode shapes represented by the curves ———, ·············, —–—, – – – – –, and —·—·—·, respectively: (a) *uniform* beam (with $d = d_1$) without attachment, (b) *three-step* beam without attachment, (c) *three-step* beam carrying three lumped masses, (d) *three-step* beam carrying three lumped masses and three rotary inertias

3rd, 4th and 5th mode shapes are represented by the curves, ———, ·············, —–—, – – – – –, and —·—·—·, respectively. Besides, Fig. 3(a) is for the "uniform" beam (with $d = d_1$) without attachment, while Figs. 3(b)-3(d) are for the "three-step" beam without attachment, carrying three lumped masses, and carrying three lumped masses together with three rotary inertias, respectively. The lowest five mode shapes shown in Figs. 4(a)-4(d) and Figs. 5(a)-5(d) are for the C-F beam and F-C beam, respectively. Their keys are the same as those for Figs. 3(a)-3(d).

From Figs. 3(a) and 3(b) one sees that the lowest five mode shapes of the three-step beam are much different from those of the uniform beam, this is because the cross-sections of the stepped beam change from step to step. From Figs. 3(c) and 3(d) one finds that, for the same three-step beam, the lowest five mode shapes for the case of carrying three point masses together with three rotary inertias are also much different from the corresponding ones for the case of carrying three

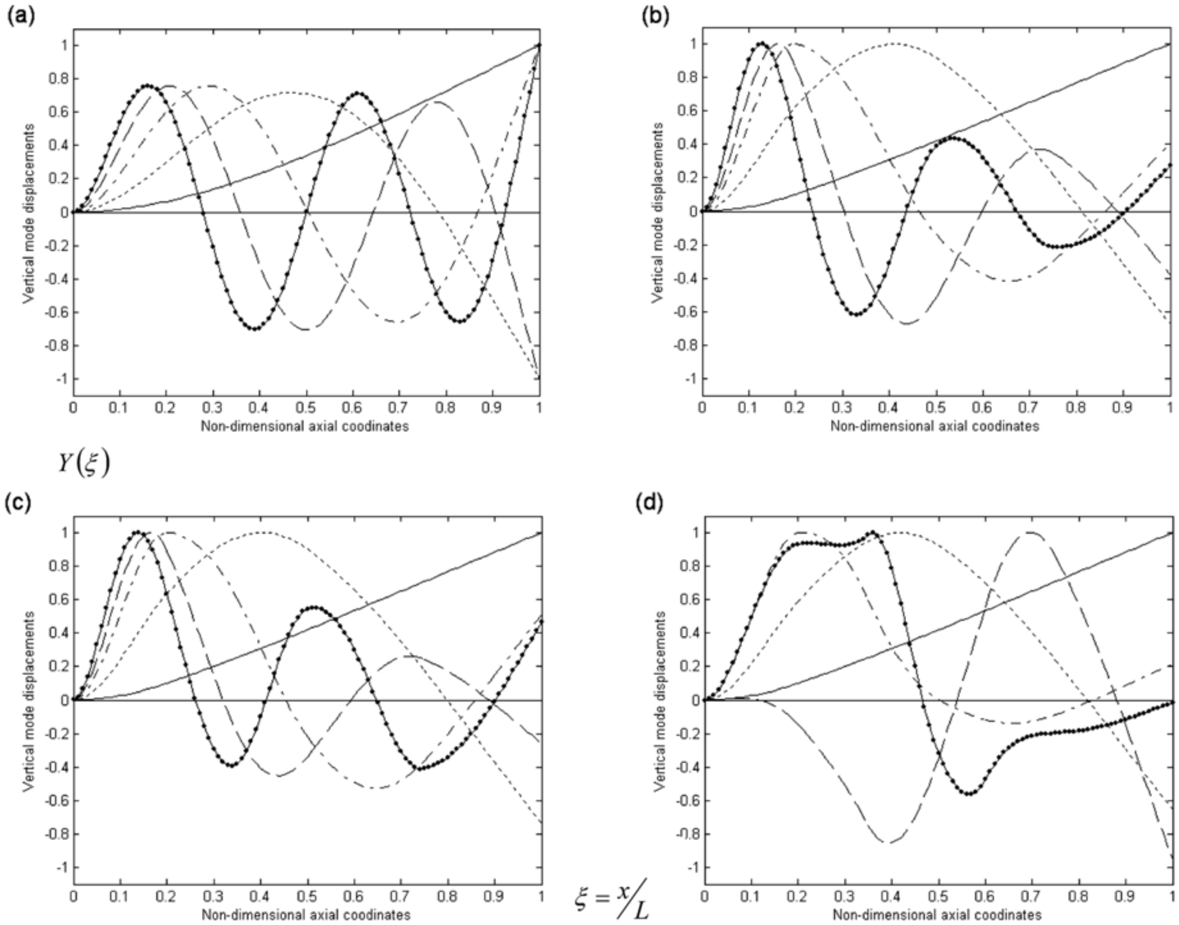

Fig. 4 The lowest five mode shapes of the C-F (clamped-free) beams: (a) for the *uniform* beam, (b)-(d) for the *three-step* beams. Key as Fig. 3

point masses only. This will be the reason why the lowest five natural frequencies of a beam carrying three point masses together with three rotary inertias are much different from the corresponding ones of the same beam carrying three point masses only as one may see from Table 5. The foregoing conclusions obtained from Figs. 3(a)-3(d) are also available for Figs. 4 and 5.

5. Conclusions

From this study the following concluding remarks can be made.

1. The stepped beam is one of the important structures in engineering. Because the literature regarding the "exact" values for the natural frequencies and associated mode shapes of a multiple-step beam carrying a number of concentrated elements is rare, the theory and the exact solutions for the examples presented in this paper will be useful for checking the accuracy of the numerical results obtained from various "approximate" methods.

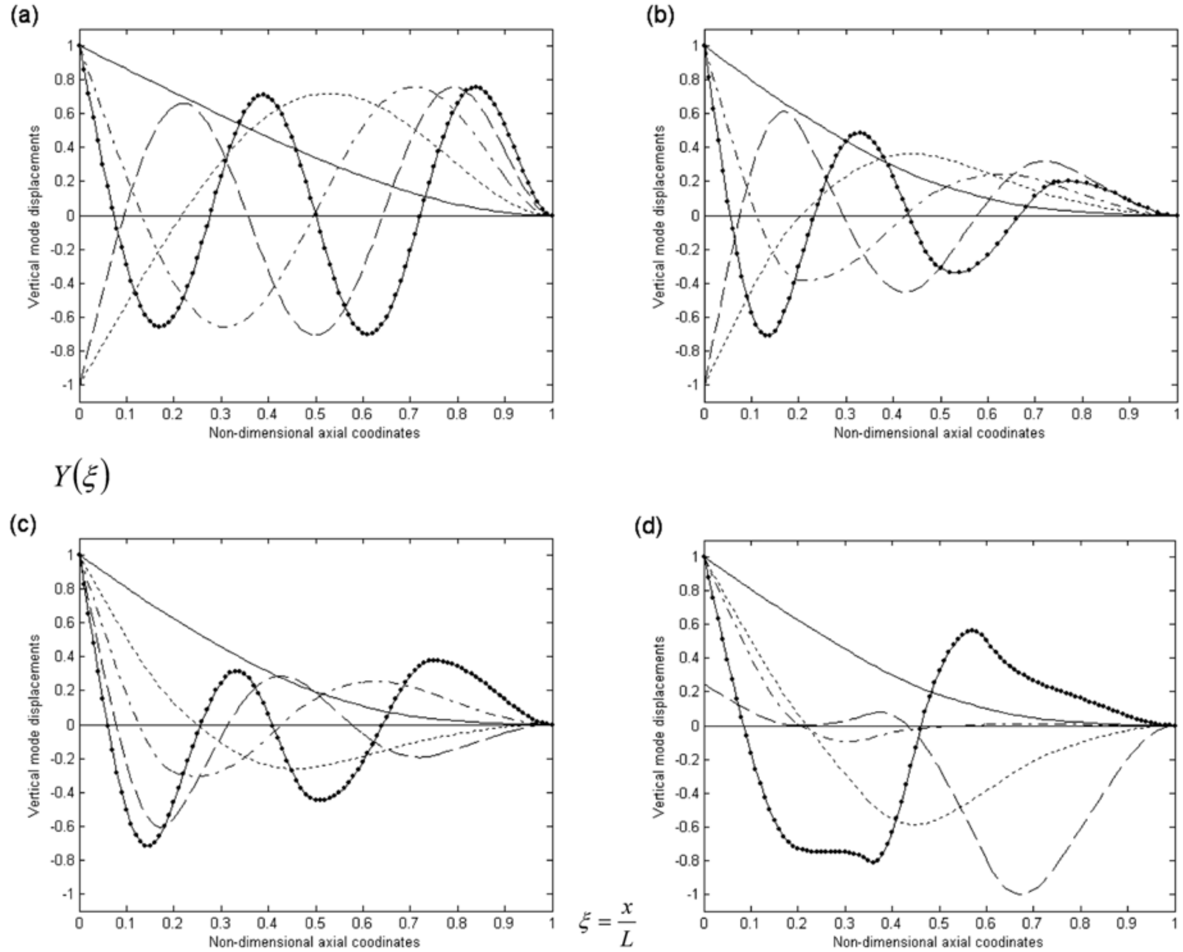

Fig. 5 The lowest five mode shapes of the F-C (free-clamped) beams: (a) for the *uniform* beam, (b)-(d) for the *three-step* beams. Key as Fig. 3

2. For a "uniform" beam, its natural frequencies and associated mode shapes in the C-F (clamped-free) condition are the same as those in the F-C (free-clamped) condition, but this is not true for a "stepped" beam. Because the natural frequencies of a stepped beam in C-F condition are much different from those in F-C condition, so are the corresponding mode shapes.
3. Because the rotary inertias have significant influence on the lowest five natural frequencies of the P-P (pinned-pinned), C-F or F-C beam, the lowest five natural frequencies and the associated mode shapes of a P-P, C-F or F-C beam carrying a number of point masses together with their rotary inertias are much different from the corresponding ones of the same beam carrying the same point masses only.
4. It is believes that, if the gyroscopic effect is negligible, the technique introduced in this paper can also be applied to determining the critical speed of the stepped shafts.

References

Balasubramanian, T.S. and Subramanian, G. (1985), "On the performance of a four-degree-of-freedom per node element for stepped beam analysis and higher frequency estimation", *J. Sound Vib.*, **99**(4), 563-567.

Balasubramanian, T.S., Subramanian, G. and Ramani, T.S. (1990), "Significance of very high order derivatives as nodal degrees of freedom in stepped beam vibration analysis", *J. Sound Vib.*, **137**(2), 353-356.

Chen, D.W. and Wu, J.S. (2002), "The exact solutions for the natural frequencies and mode shapes of non-uniform beams with multiple spring-mass system", *J. Sound Vib.*, **255**(2), 299-322.

Chen, D.W. (2003), "The exact solutions for the natural frequencies and mode shapes of non-uniform beams carrying multriple various concentrated elements", *Struct. Eng. Mech.*, **16**(2), 153-176.

De Rosa, M.A. (1994), "Free vibrations of stepped beams with elastic ends", *J. Sound Vib.*, **173**(4), 557-563.

De Rosa, M.A., Belles, P.M. and Maurizi, M.J. (1995), "Free vibrations of stepped beams with intermediate elastic supports", *J. Sound Vib.*, **181**(5), 905-910.

Epperson, J.F. (2003), *An Introduction to Numerical Methods and Analysis*, John Wiley & Son, Inc.

Hamdan, M.N. and Abdel Latif, L. (1994), "On the numerical convergence of discretization methods for the free vibrations of beams with attached inertia elements", *J. Sound Vib.*, **169**(4), 527-545.

Jang, S.K. and Bert, C.W. (1989a), "Free vibrations of stepped beams: Exact and numerical solutions", *J. Sound Vib.*, **130**(2), 342-346.

Jang, S.K. and Bert, C.W. (1989b), "Free vibrations of stepped beams: Higher mode frequencies and effects of steps on frequency", *J. Sound Vib.*, **132**(1), 164-168.

Ju, F., Lee, H.P. and Lee, K.H. (1994), "On the free vibration of stepped beams", *Int. J. Solids Struct.*, **31**, 3125-3137.

Laura, P.A.A., Rossi, R.E., Pombo, J.L. and Pasqua, D. (1994), "Dynamic stiffening of straight beams of rectangular cross-section: A comparison of finite element predictions and experimental results", *J. Sound Vib.*, **150**(1), 174-178.

Lee, J. and Bergman, L.A. (1994), "Vibration of stepped beams and rectangular plates by an elemental dynamic flexibility method", *J. Sound Vib.*, **171**(5), 617-640.

Lin, S.Y. and Tsai, Y.C. (2005), "On the natural frequencies and mode shapes of a uniform multi-span beam carrying multiple point masses", *Struct. Eng. Mech.*, **21**(3), 351-367.

Maurizi, M.J. and Belles, P.M. (1994), "Natural frequencies of one-span beams with stepwise variable cross-section", *J. Sound Vib.*, **168**(1), 184-188.

Naguleswaran, S. (2002a), "Natural frequencies, sensitivity and mode shape details of an Euler-Bernoulli beam with one-step change in cross-section and with ends on classical supports", *J. Sound Vib.*, **252**(4), 751-767.

Naguleswaran, S. (2002b), "Vibration of an Euler-Bernoulli beam on elastic end supports and with up to three step changes in cross-section", *Int. J. Mech. Sci.*, **44**, 2541-2555.

Subramanian, G. and Balasubramanian, T.S. (1987), "Beneficial effects of steps on the free vibration characteristics of beams", *J. Sound Vib.*, **118**(3), 555-560.

Wu, J.S. and Chen, D.W. (2001), "Free vibration analysis of a Timoshenko beam carrying multiple spring-mass systems by using the numerical assembly technique", *Int. J. Numer. Methods Eng.*, **50**, 1039-1058.

Wu, J.S. and Chou, H.M. (1998), "Free vibration analysis of a cantilever beams carrying any number of elastically mounted point masses with the analytical-and-numerical-combined method", *J. Sound Vib.*, **213**(2), 317-332.

Wu, J.S. and Chou, H.M. (1999), "A new approach for determining the natural frequencies and mode shapes of a uniform beam carrying any number of sprung masses", *J. Sound Vib.*, **220**(3), 451-468.

Appendix

The coefficient matrix $[B_p]$ for Eq. (14) is given by

$$[B_p] = \begin{array}{cc} \begin{array}{cccccccc} 4P-3 & 4P-2 & 4P-1 & 4P & 4P+1 & 4P+2 & 4P+3 & 4P+4 \end{array} & \\ \left[\begin{array}{cccccccc} \mathrm{s}\,\theta_{v,p} & \mathrm{c}\,\theta_{v,p} & \mathrm{sh}\,\theta_{v,p} & \mathrm{ch}\,\theta_{v,p} & -\mathrm{s}\,\theta_{v,p+1} & -\mathrm{c}\,\theta_{v,p+1} & -\mathrm{sh}\,\theta_{v,p+1} & -\mathrm{ch}\,\theta_{v,p+1} \\ \Omega_{v,p}\mathrm{c}\,\theta_{v,p} & -\Omega_{v,p}\mathrm{s}\,\theta_{v,p} & \Omega_{v,p}\mathrm{ch}\,\theta_{v,p} & \Omega_{v,p}\mathrm{sh}\,\theta_{v,p} & -\Omega_{v,p+1}\mathrm{c}\,\theta_{v,p+1} & \Omega_{v,p+1}\mathrm{s}\,\theta_{v,p+1} & -\Omega_{v,p+1}\mathrm{ch}\,\theta_{v,p+1} & -\Omega_{v,p+1}\mathrm{sh}\,\theta_{v,p+1} \\ -\Omega_{v,p}^2\mathrm{s}\,\theta_{v,p}+\alpha_p\Omega_{v,p}^5\mathrm{c}\,\theta_{v,p} & -\Omega_{v,p}^2\mathrm{c}\,\theta_{v,p}-\alpha_p\Omega_{v,p}^5\mathrm{s}\,\theta_{v,p} & \Omega_{v,p}^2\mathrm{sh}\,\theta_{v,p}+\alpha_p\Omega_{v,p}^5\mathrm{ch}\,\theta_{v,p} & \Omega_{v,p}^2\mathrm{ch}\,\theta_{v,p}+\alpha_p\Omega_{v,p}^5\mathrm{sh}\,\theta_{v,p} & \varepsilon_p\Omega_{v,p+1}^2\mathrm{s}\,\theta_{v,p+1} & \varepsilon_p\Omega_{v,p+1}^2\mathrm{c}\,\theta_{v,p+1} & -\varepsilon_p\Omega_{v,p+1}^2\mathrm{sh}\,\theta_{v,p+1} & -\varepsilon_p\Omega_{v,p+1}^2\mathrm{ch}\,\theta_{v,p+1} \\ \sigma_p\Omega_{v,p}^4\mathrm{s}\,\theta_{v,p}-\Omega_{v,p}^3\mathrm{c}\,\theta_{v,p} & \sigma_p\Omega_{v,p}^4\mathrm{c}\,\theta_{v,p}+\Omega_{v,p}^3\mathrm{s}\,\theta_{v,p} & \sigma_p\Omega_{v,p}^4\mathrm{sh}\,\theta_{v,p}+\Omega_{v,p}^3\mathrm{ch}\,\theta_{v,p} & \sigma_p\Omega_{v,p}^4\mathrm{ch}\,\theta_{v,p}+\Omega_{v,p}^3\mathrm{sh}\,\theta_{v,p} & \varepsilon_p\Omega_{v,p+1}^3\mathrm{c}\,\theta_{v,p+1} & -\varepsilon_p\Omega_{v,p+1}^3\mathrm{s}\,\theta_{v,p+1} & -\varepsilon_p\Omega_{v,p+1}^3\mathrm{ch}\,\theta_{v,p+1} & -\varepsilon_p\Omega_{v,p+1}^3\mathrm{sh}\,\theta_{v,p+1} \end{array}\right] & \begin{array}{c} 4P-1 \\ 4P \\ 4P+1 \\ 4P+2 \end{array} \end{array} \tag{A1}$$

$$\theta_{v,p} = \Omega_{v,p}\xi_p, \quad \mathrm{s}\,\theta_{v,p} = \sin\theta_{v,p}, \quad \mathrm{c}\,\theta_{v,p} = \cos\theta_{v,p}, \quad \mathrm{sh}\,\theta_{v,p} = \sinh\theta_{v,p}, \quad \mathrm{ch}\,\theta_{v,p} = \cosh\theta_{v,p}$$

$$\theta_{v,p+1} = \Omega_{v,p+1}\xi_p, \quad \mathrm{s}\,\theta_{v,p+1} = \sin\theta_{v,p+1}, \quad \mathrm{c}\,\theta_{v,p+1} = \cos\theta_{v,p+1}, \quad \mathrm{sh}\,\theta_{v,p+1} = \sinh\theta_{v,p+1}, \quad \mathrm{ch}\,\theta_{v,p+1} = \cosh\theta_{v,p+1} \tag{A2}$$

$$\alpha_p = -J_p^*\left(\frac{\overline{m}_1}{\overline{m}_p}\right), \quad \sigma_p = m_p^*\left(\frac{\overline{m}_1}{\overline{m}_p}\right), \quad \varepsilon_p = \frac{I_{p+1}}{I_p} \tag{A3}$$